scientific reports

Check for updates

OPEN

Efficient pressure regulation in nonlinear shell-and-tube steam condensers via a Novel TDn(1 + PIDn) controller and DCSA algorithm

Mostafa Jabari[1], Serdar Ekinci[2], Davut Izci[2,3], Mohit Bajaj[4,5,6]✉, Vojtech Blazek[7] & Lukas Prokop[7]

Steam condensers are vital components of thermal power plants, responsible for converting turbine exhaust steam back into water for reuse in the power generation cycle. Effective pressure regulation is crucial to ensure operational efficiency and equipment safety. However, conventional control strategies, such as PI, PI-PDn and FOPID controllers, often struggle to manage the nonlinearities and disturbances inherent in steam condenser systems. This paper introduces a novel multistage controller, TDn(1 + PIDn), optimized using the diligent crow search algorithm (DCSA). The proposed controller is specifically designed to address system nonlinearities, external disturbances, and the complexities of dynamic responses in steam condensers. Key contributions include the development of a flexible multi-stage control framework and its optimization via DCSA to achieve enhanced stability, faster response times, and reduced steady-state errors. Simulation results demonstrate that the TDn(1 + PIDn) controller outperforms conventional control strategies, including those tuned with advanced metaheuristic algorithms, in terms of settling time, overshoot, and integral of time weighted absolute error (ITAE). This study marks a significant advancement in pressure regulation strategies, providing a robust and adaptive solution for nonlinear industrial systems.

Keywords Nonlinear control, Steam condensers, Pressure regulation, PID controller, Crow search algorithm (CSA), DCSA optimization, Thermal power plant, Multistage TDn(1 + PIDn) controller

List of symbols

PI	Proportional-integral
PD	Proportional derivative
PID	Proportional-integral-derivative
TDn	Tilt-derivative with an N filter
FOPID	Fractional order PID
PIDn	Proportional integral derivative with derivative filter
DCSA	Diligent crow search optimization algorithm
CSA	Crow search optimization
EEFO	Electric eel foraging optimization
GEO	Golden eagle optimization
QIO	Quadratic interpolation optimization
KMA	Komodo mlipir algorithm
GA	Genetic algorithm
CSA	Cooperation search algorithm

[1]Faculty of Electrical Engineering, Sahand University of Technology, Tabriz, Iran. [2]Department of Computer Engineering, Batman University, Batman, Turkey. [3]Applied Science Research Center, Applied Science Private University, Amman 11931, Jordan. [4]Department of Electrical Engineering, Graphic Era (Deemed to be University), Dehradun 248002, India. [5]College of Engineering, University of Business and Technology, Jeddah 21448, Saudi Arabia. [6]Graphic Era Hill University, Dehradun 248002, India. [7]ENET Centre, VSB—Technical University of Ostrava, Ostrava 708 00, Czech Republic. ✉email: thebestbajaj@gmail.com

en-CSA	Enhanced version of the cooperation search algorithm
GWO	Gray wolf optimization
PSO	Particle swarm optimization
SMA	Slime mould algorithm
ITAE	Integral of time weighted absolute error
G_s	Steam content on the shell side
G_{st}	Exhaust steam volume from the turbine
G_{ost}	Additional steam inlet to the condenser
G_c	Main steam condensate
G_{ss}	Amount of steam removed by vacuum pumps
P_s	Internal pressure of steam in the condenser
R_s	Steam gas constant
V	Gas volume inside the condenser
T_s	Temperature of the saturated gas
H_s	Average steam enthalpy
H_{st}	Enthalpy of the steam turbine exhaust
H_{ost}	Enthalpy of any other steam inlets
G_{vb}	Amount of air entering the condenser from the vacuum break valve
G_n	Air volume from normal drainage condensation
G_g	Air introduced through seal leakage
G_a	Air extracted by the air removal system
P_a	Air pressure inside the condenser
R_a	Gas constant for air
P_c	Absolute pressure
L_c	Water level in the hot well
G_w	Quality of the hot well water
$\boldsymbol{\rho}$	Density of the hot well water
A_w	Cross-sectional area of the hot well
G_p	Volume of oxygen expelled through bubbling
G_{wo}	Quantity of water exiting the condenser
H_p	Enthalpy of the oxygen exhaust steam
H_w	Enthalpy of the hot well water
H_w	Enthalpy of the saturated water corresponding to the condenser pressure
M_w	Quantity of circulating water
$_{Cp}$	Heat capacity of the circulating water
Q	Heat from the steam outlet
Q_w	Amount of heat absorbed by the circulating water
U	Heat transfer coefficient of the condenser
K_D, K_{DD}, K_P, K_I	Derivative, proportional and integral gains of controller
OS, T_P, T_r, T_s	Overshoot, Peak time, Rise time, Settling time
$\boldsymbol{\Delta t_m}$	Logarithmic mean temperature difference
N, NN, n	Controller filter
A	Heat transfer area of the condenser
HO	Hippopotamus optimization
e_p	Elimination phase
e_t	Elimination percent
T_h	Threshold
$\boldsymbol{\omega}$	Inertial coefficient
OF	Objective function
t_{fult}, t_{sim}	Simulation time
F_{cw}	Flow rate of the circulating water
PSO	Particle swarm optimization
λ, μ	Integral and derivative order
$\boldsymbol{\delta t}$	Heat transfer error of the condenser
ITAE	Integral of time weighted absolute error
T_{cw}	Inlet temperature of the circulating water
T	Outlet temperature of the circulating water
$\boldsymbol{\Lambda}$	Latent heat of vaporization
$\boldsymbol{\beta}$	Temperature constant
$\boldsymbol{\alpha}$	Temperature coefficient per pressure unit
$\boldsymbol{\alpha}_1, \boldsymbol{\alpha}_2$	Coefficient for first and second variable term
N(s)	Noise signal
P(s)	Condenser pressure
U(s)	Output signal from proposed controller
E(s)	Error between pressure setpoint and condenser
R(s)	Pressure setpoint
$\boldsymbol{\Delta U(s)}$	Controller output signal
$\boldsymbol{\Delta U_1(s)}$	Multi stage controller's initial stage control signal

Efficient pressure regulation within steam condensers is critical for maintaining optimal performance in thermal power plants[1]. These condensers play an essential role by converting exhaust steam from turbines back into water, enabling its recirculation in the power generation process[2,3]. Traditional control methods, such as proportional-integral (PI)[4], and fractional-order PID (FOPID)[5], are widely employed for pressure regulation. However, these methods frequently encounter challenges when addressing system nonlinearities and external disturbances, which can degrade performance and jeopardize equipment safety[6,7]. To overcome these limitations, we present a novel multistage controller, TDn(1 + PIDn), optimized using the diligent crow search algorithm (DCSA). This controller is specifically designed to handle the complexities associated with nonlinear shell-and-tube steam condensers, ensuring enhanced stability and control precision under various operational conditions[8].

In recent studies, a variety of optimization algorithms have been employed to tune controllers for industrial applications. For instance, the slime mould algorithm (SMA)[9], inspired by the natural behavior of slime molds, is another bio-inspired algorithm that has proven effective for controller tuning in nonlinear systems. Additionally, algorithms like the golden eagle optimizer (GEO)[10], which emulates the hunting behavior of golden eagles, and the komodo mlipir algorithm (KMA)[11], based on the movement of Komodo dragons, have shown success in optimizing control parameters. Other advanced optimization techniques include the quadratic interpolation optimization (QIO)[12], grey wolf optimizer (GWO)[13], and particle swarm optimization (PSO)[14], all of which have been applied to enhance PI and PID control strategies. These algorithms leverage various natural and mathematical principles to efficiently explore complex optimization landscapes, providing better parameter tuning than traditional approaches[15,16].

In addition to optimization algorithms, several controllers have been applied to steam condenser systems to improve pressure regulation. The FOPID controller, optimized with en-CSA[8], has been utilized to regulate shell-and-tube heat exchangers, demonstrating the adaptability and strength of fractional-order controllers in challenging industrial settings. Furthermore, controllers such as the fuzzy self-tuning PI controller offer adaptive capabilities, enabling real-time adjustments based on system behavior[17]. Traditional controllers like the PID and PI remain widely used for their simplicity and effectiveness[18–21], while the PD controller, often combined with filters to mitigate noise, provides a faster response in transient conditions[22]. These controllers, alongside modern optimization algorithms, offer diverse solutions to meet the specific needs of nonlinear systems like steam condensers, aircrafts and DC motors[23–30].

A wealth of literature underscores the significance of advanced controllers and optimization algorithms in managing nonlinear systems such as steam condensers. In the study by Li and Wang[17], a GWO method was used to tune a PI controller for a steam condenser. This approach showed notable improvements in stability and response speed compared to other algorithms like PSO and GA. Another study by Jibril, et al.[31] explored the effectiveness of a fuzzy self-tuning PI controller in a shell-and-tube condenser system, highlighting that fuzzy logic enhances adaptability and control accuracy, providing a robust solution for varying operational conditions . Alzakari, et al.[8] presented an en-CSA to optimize a FOPID controller. This study showed that en-CSA achieved faster settling times, reduced overshoot, and improved stability, surpassing conventional tuning methods in handling nonlinear condenser systems. These findings collectively emphasize the growing importance of bio-inspired optimization algorithms and advanced control structures, paving the way for more resilient and efficient pressure regulation solutions in steam condensers. The main findings from these recent studies are summarized in Table 1.

The key contributions of this paper are as follows:

- This research introduces a multi-stage TDn(1 + PIDn) controller, uniquely tailored for managing pressure in the nonlinear dynamics of a shell-and-tube steam condenser. This advanced controller structure provides superior flexibility and control precision in handling the system's intricate thermal behavior.
- Through optimization using the DCSA, the TDn(1 + PIDn) controller outperforms traditional control methods, showing marked improvements in stability, accuracy, and response speed, even under challenging operational scenarios.
- The controller's performance was rigorously evaluated, revealing that it significantly reduces key performance issues such as settling time, overshoot, and steady-state errors. Moreover, the reduction in ITAE (Integral of time weighted absolute error) highlights the system's ability to maintain optimal control across fluctuating conditions.
- We developed and applied DCSA as a powerful tool for optimizing controller parameters in industrial applications, particularly in thermal power systems. The findings contribute to a deeper understanding of bio-inspired optimization methods, offering a new, efficient approach for tackling complex control challenges in engineering.

Article	Controller	Optimizer	Advantages	Disadvantages	Key Findings
Li and Wang[17]	PI controller	GWO	Improved performance over manual tuning methods	Computationally intensive, potential for local optima	GWO-tuned PI controller significantly improves condenser pressure control performance.
Jibril, et al.[31]	Fuzzy self-tuning PI Controller	Fuzzy logic tuning	Adapts to dynamic changes, maintains system stability	Complexity in controller design	Fuzzy self-tuning PI controller enhances system adaptability and stability.
Alzakari, et al.[8]	FOPID controller	en-CSA	Fast convergence rate, accurate pressure control, improved stability	Increased computational cost, complex tuning	en-CSA optimized FOPID controller achieves superior stability and response time.

Table 1. Summary of the utilization of controllers and optimization methods in recent studies.

The structure of the paper is as follows: Sect. 2 covers the dynamic modeling of the shell-and-tube steam condenser system, providing a detailed explanation of its nonlinear behavior. In Sect. 3, we present the design and development of the multi-stage TDn(1 + PIDn) controller, optimized using DCSA. Section 4 discusses the DCSA optimization method, highlighting its suitability for parameter tuning. Section 5 showcases the simulation results and offers a comprehensive comparison with other popular controllers and meta-heuristic optimization methods. Finally, Sect. 6 concludes the paper with a summary of key findings and potential future directions.

Mathematical modeling of shell-and-tube steam condenser

The dynamic behavior of a shell-and-tube steam condenser can be modeled by analyzing the interaction between steam, cooling water, and the heat exchange surfaces within the system[32]. As can be seen in Fig. 1, the shell-and-tube condenser normally has an exterior design that is either cylindrical or elliptical in shape. It is equipped with end closures that are designed to create water chambers, and it is positioned with a perforated tube plate in between the closures and the basic shell. The many cooling water pipes that are organized in layers are held in place by this plate. Through a pipe located at the top of the condenser, steam is introduced into the device. This pipe is connected to the exhaust equipment either directly or indirectly through a compensator. Condensed water is collected at the bottom of the shell in a tank, and air is expelled through an outlet near the lower section.

The condenser works by allowing steam to flow in through the inlet pipe, where it condenses upon coming into contact with the cooler tube walls. During this process, the steam transfers its heat to the cooling water inside the pipes. The cooling water, which enters at a specific temperature, flows through the first set of pipes at the bottom of the condenser. As it moves through additional chambers and pipes, the water absorbs heat from the steam. After several stages, the now-warmed cooling water exits through the outlet pipes at a higher temperature, completing the heat exchange process. The constant condensation of steam in the mixture steadily lowers the quality of the steam as it moves toward the exhaust port, while the air content gradually increases. This occurs as the steam and air flow toward the exhaust port. When the air concentration in the mixture that is entering the cooling zone reaches a significant level, the condensation process is said to have reached its conclusion.

The shell-and-tube condenser's behavior can be modeled mathematically, with the governing equations for the steam zone provided in[17,19].

$$\frac{dG_s}{dt} = G_{st} + G_{ost} + G_c - G_{ss} \tag{1}$$

$$\frac{dP_s}{dt} = \frac{R_s\left(\frac{dG_s}{dt}\right)}{V}(T_s + 273.15) \tag{2}$$

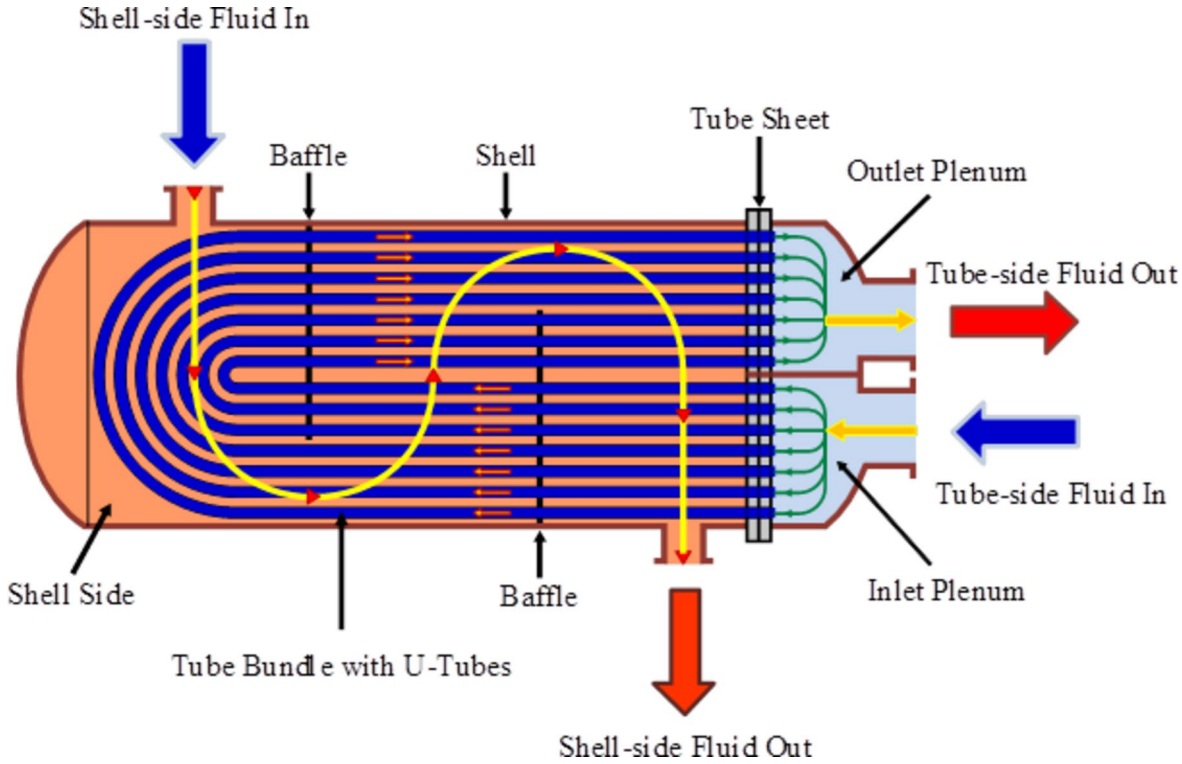


Fig. 1. General schematic of shell-and-tube steam condenser.

$$\frac{dG_sH_s}{dt} = G_{st} \times H_{st} + G_{ost} \times H_{ost} - (G_c + G_{ss}) \times H_s \tag{3}$$

The steam mass balance, vapor pressure, and average steam enthalpy in the condenser are all aspects that are addressed by Eqs. (1), (2) and (3). Related references[17,19] contain the governing equations that correspond to the air zone which can be found in those references.

$$\frac{dG_a}{dt} = G_{vb} + G_n + G_g - G_a \tag{4}$$

$$\frac{dP_a}{dt} = \frac{R_a\left(\frac{dG_a}{dt}\right)}{V}(T_s + 273.15) \tag{5}$$

$$P_C = P_s + P_a \tag{6}$$

The air mass balance, air pressure, and absolute pressure within the condenser are all described by the Eqs. (4), (5) and (6). In the hot water zone, the equations that regulate the zone are described in[17,19].

$$L_c = \frac{G_w}{\rho\, A_w} \tag{7}$$

$$\frac{dG_w}{dt} = G_c + G_{gp} - G_{wo} \tag{8}$$

$$\frac{dG_wH_w}{dt} = G_c \times H_{cw} + G_{gp} \times H_{gp} - (G_{wo} \times H_w) \tag{9}$$

The hot well water level equation, the hot well water quality equation, and the hot well water enthalpy equation are each represented by the Eqs. (7), (8) and (9), respectively. Using the dynamic heat balance equation for the flowing water, the mathematical model for the condenser tube side is created. This equation is described in[17,19].

$$M_wC_w\frac{dT_2}{d_t} = Q - Q_w = UA\Delta\, t_m - F_{cw}C_p(T - T_{cw}) \tag{10}$$

The value of Δt_m is calculated as follows, based on[17,19].

$$\Delta\, t_m = \frac{T - T_{cw}}{\ln\left[\frac{(T_s - T_{cw})}{(T_s - T)}\right]} \tag{11}$$

The degree of overcooling in the condenser is calculated as $\Delta t_m = T_c - T_w$, where T_c is the saturated water temperature corresponding to the vapor pressure in the condenser, and T_w is the temperature of the hot well water in the condenser. The heat transfer error in the condenser is defined as $\delta t = T_s - T$, where T_s is the saturated gas temperature corresponding to the saturation pressure in the condenser. For the dynamic heat balance, it is assumed that the total condensation rate remains constant, and that both the incoming steam and the outgoing condensate are in a saturated state. Consequently, the thermal energy transferred from the steam to the circulating water is equivalent to the steam's heat potential. The heat released by the steam can be calculated using the following equations:

$$\frac{dT}{dt} = \frac{F_{cw}}{M_{cw}}(T_{cw} - T) + \frac{Q}{M_{cw}C_p} \tag{12}$$

To ensure that the mass balancing of steam and condensate is carried out in an accurate manner, it is essential to have a continuous system that maintains a steady volume of both steam and air. This must be done in order to guarantee that the mass balancing is carried out. Through the use of this, it is feasible to guarantee that the mass balance is carried out. This particular facet is one of the things that is taken into consideration to some degree. To put it another way, it is vital to restrict the outflow of condensate within a particular range in order to maintain the appropriate amount of vapor condensation within the condenser (at a particular vacuum level). In order to regulate the amount of condensation that takes place, this operation is carried out. It is essential to do this in order to maintain a consistent level of the necessary quantity of vapor condensation. It is necessary to take this step in order to guarantee that the condenser will be able to keep the required amount of vacuum during its operation. For the purpose of simplifying the model, we will make the assumption that the condensate will be in a saturated condition both when it enters the system and when it leaves the system. This will allow us to simplify the model. The model will be easier to understand as a result of this. As a result, the model becomes easier to understand, and the following equation best represents the behavior of an ideal gas. This is because of the circumstances that have arisen.

$$\frac{dP}{dt} = \frac{RT_c}{V}(F_s - F_c) \tag{13}$$

Proposed multi-stage controller TDn(1 + PIDn)

The innovative TDn(1 + PIDn) controller is designed to improve the precision and speed of pressure regulation in steam condensers. The proposed controller integrates several key components, each playing a critical role in achieving optimal control performance. Below is a detailed explanation of each section of the controller:

TDn (tilt-derivative term with n filter)

The first part of the controller is the TDn component, which is a tilt-derivative with an n filter. Unlike traditional derivative terms, which solely rely on the rate of change of the error signal, the TDn term introduces nonlinear dynamics to the derivative action. This results in enhanced sensitivity to rapid changes in pressure, making the controller more reactive and capable of stabilizing the system against large fluctuations in a timely manner. This term also helps in suppressing noise amplification commonly associated with conventional derivative terms, thus improving overall system robustness.

PIDn (proportional-integral-derivative with n filter)

The second section of the controller is a PIDn block that combines proportional, integral, and derivative actions, each equipped with n filter. This approach improves the flexibility and adaptability of the PID control mechanism to handle complex dynamic responses of the steam condenser system.

- **Proportional term (P)**: The proportional gain is responsible for reducing the present error by adjusting the output based on the current difference between the setpoint and the measured pressure. By including a nonlinear gain, the proportional term becomes more effective in large error regions, allowing the controller to make aggressive corrections when necessary.
- **Integral term (I)**: The integral term eliminates steady-state errors by integrating the error signal over time. The nonlinear gain modifies the standard integral action, making it more efficient at minimizing long-term deviations while avoiding excessive overshooting, a common problem in conventional PID controllers. This nonlinear adjustment allows the controller to maintain pressure stability over extended operating periods.
- **Derivative term (D)**: The derivative term predicts future system behavior based on the rate of error change. In the PIDn section, the derivative term is similarly enhanced with a nonlinear gain, which improves the controller's foresight capabilities, resulting in smoother transitions and quicker response times when system dynamics change abruptly.

Interaction between TDn and PIDn

The interaction between the TDn and PIDn components is what sets this controller apart from traditional models. The combination of a TDn action with a PIDn block ensures that both transient and steady-state responses are managed effectively. While the TDn term ensures rapid stabilization in the face of large pressure deviations, the PIDn section fine-tunes the control output to maintain the desired setpoint over time, even in the presence of disturbances or system noise.

Multi-stage structure

The TDn(1 + PIDn) controller demonstrates a unique multi-stage design that significantly enhances its performance in managing nonlinear systems, such as shell-and-tube steam condensers. This innovative structure enables stepwise refinement of control actions, optimizing each phase of the process to address specific challenges with precision and adaptability. The initial adjustment phase focuses on rapid response, allowing the controller to swiftly mitigate disturbances or setpoint variations, effectively preventing instability and excessive oscillations. The mid-range correction phase ensures smooth transitional control by addressing moderate deviations and managing the nonlinearities inherent in complex systems. Finally, the fine-tuned stabilization phase provides precise steady-state regulation, minimizing residual errors and maintaining long-term stability even under persistent deviations.

By seamlessly integrating these stages, the TDn(1 + PIDn) controller achieves an exceptional balance between responsiveness and stability. Its ability to adapt dynamically across all phases of operation ensures superior performance compared to conventional FOPID, PI-PDn and PI controllers. This advanced control strategy not only enhances system precision but also makes the TDn(1 + PIDn) controller particularly advantageous for demanding industrial applications, such as steam condenser pressure regulation, where nonlinear behaviors and complex dynamics must be effectively managed. Figure 2 contains the block diagram that illustrates the controller that is being considered as a possible alternative.

Equation (14), which presents the open-loop transfer function for the first-stage controller, is as follows:

$$G_{TDn}(s) = \frac{\Delta U_1(s)}{\Delta \mathrm{T}(s)} = \frac{K_T}{s^{\frac{1}{n}}} + [K_D \times \left(\frac{Ns}{N+S}\right)] \tag{14}$$

Shell-and-tube steam condensers benefit from added stability and control that can be fine-tuned thanks to the second stage. Presented below is the equation that represents the open-loop transfer function of the second stage controller. (15) :

$$G_{(1+PIDn)}(s) = \frac{\Delta \mathrm{U}(s)}{\Delta U_1(s)} = 1 + [K_P + \frac{K_I}{s} + \frac{K_{DD}NNs}{s+NN}] \tag{15}$$

In order to illustrate the open-loop representation of the proposed controller, the Eq. (16) can be constructed as follows:

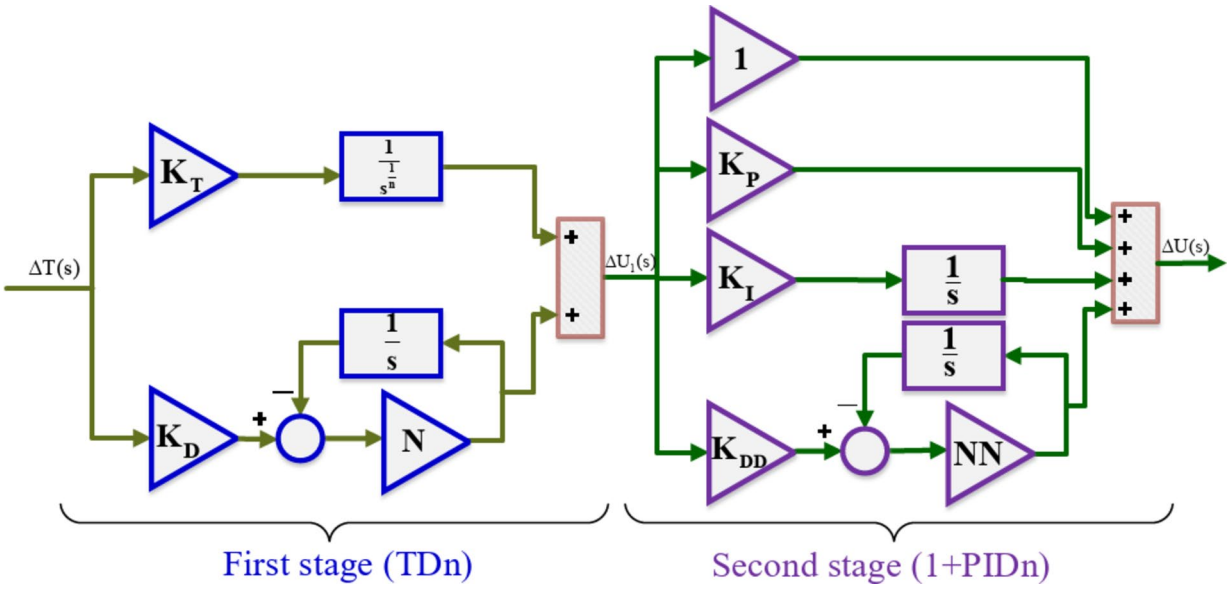


Fig. 2. Block diagram of the proposed multistage TDn(1 + PIDn) controller.

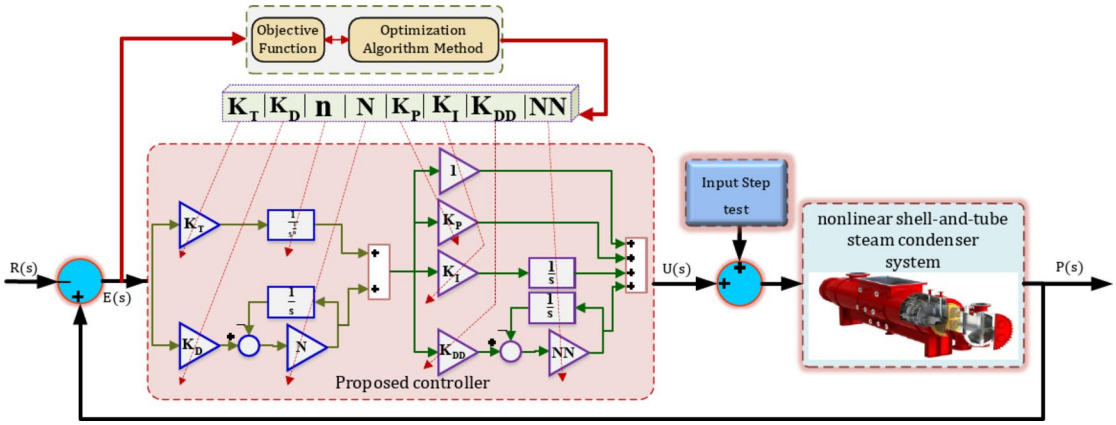


Fig. 3. Block diagram of the shell and tube steam condenser system with proposed TDn(1 + PIDn) controller.

$$G_{TDn(1+PIDn)}(s) = \frac{\Delta U(s)}{\Delta T(s)} = \left[\frac{K_T}{s^{\frac{1}{n}}} + \left(\frac{K_D N s}{N+s}\right)\right] \times \left[1 + \left(K_P + \frac{K_I}{s} + \frac{K_{DD} NN s}{s+NN}\right)\right] \quad (16)$$

Nonlinear gain tuning

One of the novel aspects of this controller design is the introduction of nonlinear gain tuning parameters for both the TDn and PIDn blocks. These parameters are carefully selected to match the dynamic properties of the steam condenser system, allowing the controller to adapt to varying operating conditions. The tuning process optimizes the balance between responsiveness and stability, ensuring efficient pressure regulation even in highly volatile environments. Figure 3 depicts the block diagram of the shell and tube steam condenser system incorporating a TDn(1 + PIDn) controller. In this diagram, $R(s)$, E (s), U (s), and $P(s)$, represent the pressure setpoint, error between pressure setpoint and condenser, output signal from proposed controller and condenser pressure, respectively. For the time being, the closed-loop reaction to a step change in the P setpoint is an approach that is being applied in order to accomplish the objectives that are related with this particular research. This particular reaction involves a transition from 90 kPa to 95 kPa.

Optimization technique

Crow search algorithm (CSA)

The crow search algorithm (CSA)[33] is a population-based metaheuristic inspired by the intelligent behavior of crows in nature, particularly their ability to hide food and remember the locations of hidden caches. Each crow in the algorithm represents a candidate solution, and its memory stores the best solution it has found so far. The

crows update their positions by following other crows or moving randomly, aiming to find the optimal solution to the problem.

The key mechanism of the CSA involves two scenarios: one where a crow follows another to its hiding place, and one where the followed crow deceives the follower by moving to a different position. Mathematically, the position update for crow *i* at iteration $t+1$ is given by:

$$x_i^{t+1} = \begin{cases} x_i + r_i \times fl_i^t \times \left(m_j^t - x_i^t\right), & if\ r_j \geq AP_j \\ Random\ position, & if\ r_j < AP_j \end{cases} \tag{17}$$

Where, x_i^t, m_j^t, r_i, r_j, fl_i^t and AP_j are the position of crow *i* at iteration *t*, memory (best-known position) of crow *j*, random numbers in the range [0, 1], flight length of crow *i* and the awareness probability of crow *j* respectively. In the first scenario, crow *i* follows crow *j* to its hiding place if $r_j \geq AP_j$. In the second scenario, crow *j* becomes aware of being followed and deceives crow *i* by moving to a random position in the search space. This mechanism allows CSA to balance between exploration (random moves) and exploitation (following better solutions).

Diligent crow search algorithm (DCSA)

The diligent crow search algorithm (DCSA) enhances the original CSA by addressing its limitations, such as slow convergence and the tendency to get stuck in local optima. DCSA introduces several modifications that improve both the exploration and exploitation capabilities of the algorithm. The main modifications include the elimination of underperforming crows and dynamic search space expansion. The main steps of DCSA algorithm are:

1. **Initialization**: Begin by generating a random population of crows, where each crow x_i^0 represents a candidate solution. Initialize each crow with its current position m_i^0.
2. **Fitness evaluation**: Evaluate the fitness of each crow using an objective function $f\left(x_i^t\right)$ that quantifies the quality of its solution. The goal is to either minimize or maximize this objective function based on the problem's requirements.
3. **Position update**: Update the position of each crow in each iteration based on whether it follows another crow or moves randomly. If a crow *j* is unaware of being followed, crow *i* moves towards *j*'s memory according to:

$$x_i^{t+1} = x_i + r_i \times fl_i^t \times \left(m_j^t - x_i^t\right) \qquad if \quad r_j \geq AP_j \tag{18}$$

If crow *j* is aware of being followed, crow *i* moves to a random position.

$$x_i^{t+1} = Random\ position, \qquad if\ r_j < AP_j \tag{19}$$

4. **Elimination phase**: After a predefined number of iterations, the algorithm eliminates a percentage e_p of the worst-performing crows. those with the lowest fitness values. These crows are replaced by new ones, randomly positioned in the search space. This phase is crucial for maintaining diversity in the population and preventing the algorithm from getting trapped in local optima. The elimination process occurs when the iteration *t* is a multiple of the elimination threshold e_t. The number of eliminated crows is determined by the elimination percentage e_p, and the new crows are introduced as:

$$x_i^{t+1} = Random\ position, \qquad \forall\, i \in\ eliminated\ set \tag{20}$$

5. **Dynamic search space expansion**: Initially, the algorithm searches within a limited region of the search space. As the iteration progresses, the search space expands dynamically. The expansion is controlled by two parameters: T_h (the threshold for space expansion) and ω (the rate of expansion). When the amplitude of a crow's parameters exceeds T_h, the search space is expanded by ω :

$$if\ \left|x_i^{t+1} - x_i^t\right| > T_h,\ \ then\ increase\ the\ search\ space\ by\ \omega \tag{21}$$

This controlled expansion ensures that the algorithm does not prematurely focus on a small region of the search space and allows it to explore larger areas as needed.

6. **Memory update**: Update each crow's memory after every iteration. If the new position x_i^{t+1} has better fitness than the current memory m_i^t, update the memory accordingly:

$$m_i^{t+1} = \begin{cases} x_i^{t+1}, & if\ f\left(x_i^{t+1}\right) < f\left(m_i^t\right), \\ m_i^t, & otherwise. \end{cases} \tag{22}$$

7. **Termination**: The algorithm stops when a termination criterion is met, such as reaching a maximum number of iterations L or achieving a satisfactory solution. The best solution found during the search is returned as the global optimum. Algorithm 1 presents the pseudocode for DCSA optimization method.

To enhance the performance of the multistage TDn(1 + PIDn) controller, the ITAE is employed as the objective function. This criterion focuses on reducing errors that persist over time, making it well-suited for assessing control system effectiveness in dynamic environments.

1. Initialize population of crows, Position[*i*], for $i = 1$ to N (randomly within the search space).
2. Set memory for each crow: Memory[*i*] = Position[*i*].
3. Evaluate fitness for each crow: Fitness[*i*] = f(Position[*i*]).
4. Set best position as the best current position among all crows based on fitness.
5. Set iteration counter $t = 1$.
6. While $t \leq$ Max Iteration do:
a. For each crow *i*:
i. Select a random crow *j* (where $j \neq i$).
ii. Generate a random number $r \in [0, 1]$.
iii. If $r \geq AP_j$ (awareness probability of crow *j*):
- Update position: Position[*i*] = Position[*i*] + r × *fl* × (Memory[*j*] - Position[*i*]).
iv: Else: Move crow *i* to a random position in the search space.
b. Evaluate fitness Fitness[*i*] = f(Position[*i*]).
c. Update memory: If Position[*i*] is better than Memory[*i*], update Memory[*i*] = Position[*i*].
d. Update best position: If Position[*i*] is better than best position, update best position = Position[*i*].
e. Elimination Phase (every *et* iterations):
- If *t* % *et* == 0: Sort population by fitness, eliminate the worst *ep*%, and replace with new random positions.
f. Dynamic search space expansion:
- If the change in position |Position[*i*] - Memory[*i*]| exceeds a predefined threshold T_h, expand the search space by a factor ω.
7. Increment iteration counter $t = t + 1$.
8. End while.
9. Return best position as the optimal solution.

Algorithm 1. Pseudo-code of the proposed method.

The ITAE objective function (OF), as defined in Eq. (23), was applied for this purpose.

$$OF_{ITAE} = \int_{y}^{x} |e(t)|\,(t-y)dt \tag{23}$$

Here, $x = t_{sim} = 50$ seconds represents the total simulation time, and $y = t_{fult} = 10$ seconds marks the point when a disturbance (or fault) is introduced. This function plays a crucial role in the optimization process by guiding the DCSA to adjust the controller parameters in a way that minimizes the overall error, particularly during critical periods after a disturbance occurs. The optimization of the multistage TDn(1+PIDn) controller's parameters is constrained by predefined boundaries, as shown in Table 2. These gain boundaries are selected based on the physical characteristics of the steam condenser system and the desired performance goals, ensuring that the search space remains both feasible and efficient.

The proposed DCSA-based TDn(1 + PIDn) controller is implemented in the steam condenser system, as depicted in Fig. 4. The figure illustrates the process flow, beginning with the initialization of the crows' population and the configuration of control parameters for pressure regulation.

The DCSA optimization algorithm was executed in ten separate rounds, with Table 3 displaying the best, worst, and average OF values achieved by different optimization methods. Figure 5 compares the effectiveness of five algorithms: DCSA, hippopotamus optimization (HO)[34], golden eagle optimization (GEO)[10], CSA, RIME optimization algorithm (RIME)[35–37], and PSO[14] in minimizing the OF, using boxplots. The boxplot in Fig. 5 clearly demonstrates that the poorest outcome from the DCSA algorithm surpasses the best results of the other four algorithms, emphasizing the DCSA algorithm's superior performance.

Iterations of the DCSA algorithm were carried out for a substantial amount of time in order to ensure that the algorithm would eventually reach the optimal point. For the purpose of determining whether or not the suggested controller is effective, the DCSA technique is utilized. The results of this optimized technique are depicted in Fig. 6. This approach produces the lowest OF values after 100 iterations, which demonstrates the controller's outstanding performance. Finally, Table 4 shows the optimal controller parameter values in nonlinear shell-and-tube steam condenser obtained from the best results produced by the DCSA algorithm.

Gains	K_T	K_D	*n*	*N*	K_P	K_I	K_{DD}	NN
Lower limit(min)	1	1	0	1	1	1	1	1
Upper limit(max)	20	6	0.001	1000	50	6	6	1000

Table 2. Range of gains in proposed controller.

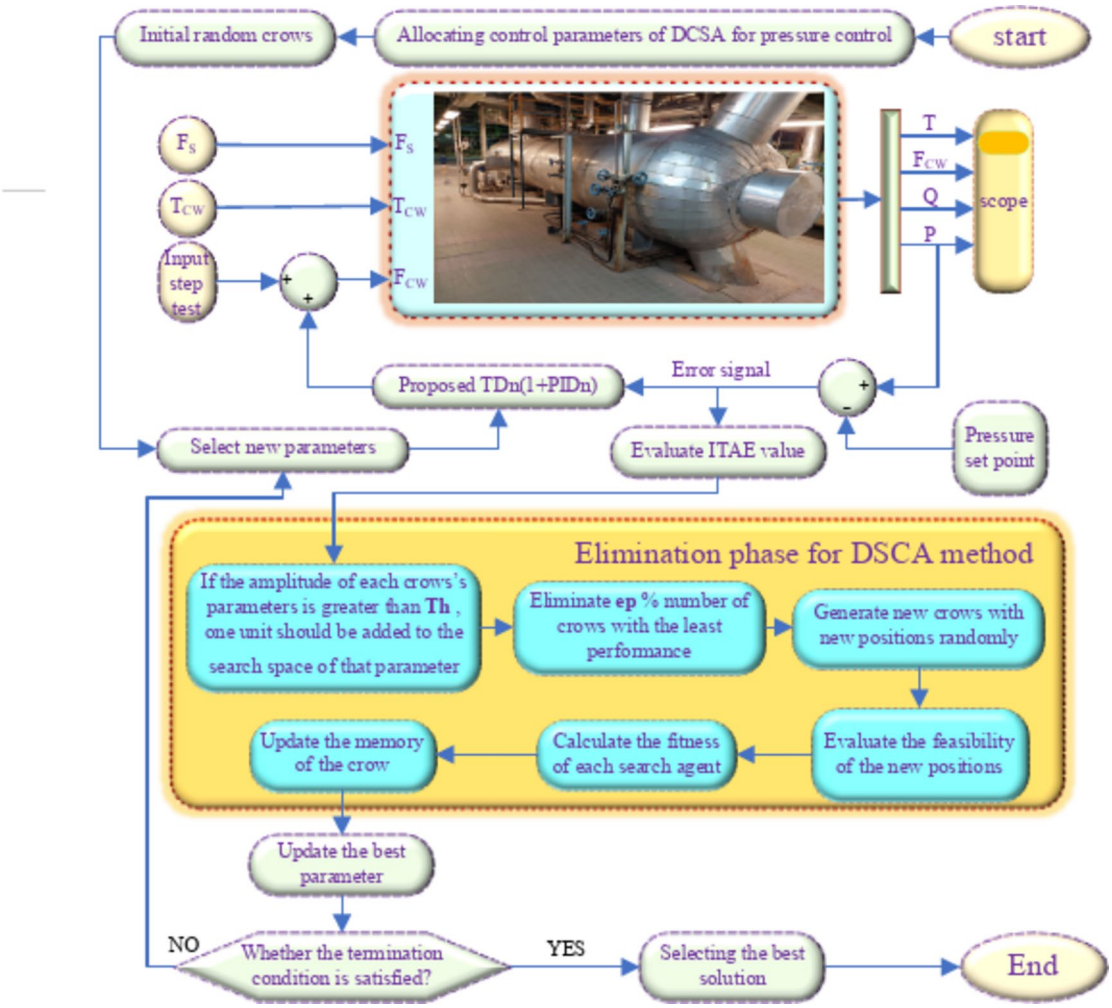


Fig. 4. Flowchart of the proposed TDn(1 + PIDn) controller tuned by DCSA to steam condenser.

Algorithm	DCSA	HO	CSA	RIME	PSO
Best	1.5212	1.9899	2.1216	2.1100	7.3618
Worst	4.7496	5.9415	8.1469	8.5050	10.7816
Mean	2.2103	3.0021	5.3416	5.1637	9.0849

Table 3. Results of the OF after ten iterations of optimization algorithms using the TDn(1 + PIDn) controller.

Results of the simulation and analysis

Parameters of the nonlinear shell-and-tube steam condenser under examination

Before continuing with the analysis and presenting the findings of the simulation, it is necessary to first determine the significant factors and variables that describe the steam condenser system that is being examined. This is a vital step. Table 5 offers a comprehensive overview of these elements, each of which plays a critical role in accurately representing and assessing the system's performance. The assigned parameter values, along with their respective units, are documented within the table for reference.

From a scientific point of view, these characteristics consist of essential components such as heat transfer coefficients, steam flow rates, condenser pressure, and cooling water temperature, amongst other things. The dynamic behavior and overall performance of the steam condenser system are both highly impacted by each of the factors taken into consideration. For example, the heat transfer coefficient has a direct influence on the efficiency of heat exchange between the steam and the cooling water, which in turn has an effect on the thermal performance of the condenser.

To effectively simulate the system's response to various control strategies, it is essential to have a solid grasp of these parameters from a physical point of view. When it comes to the efficiency with which the steam condenses and transmits heat to the cooling water, the heat transfer coefficient is the crucial factor. It is possible for variations in steam flow rates to have an effect on the pressure and temperature inside the condenser, which

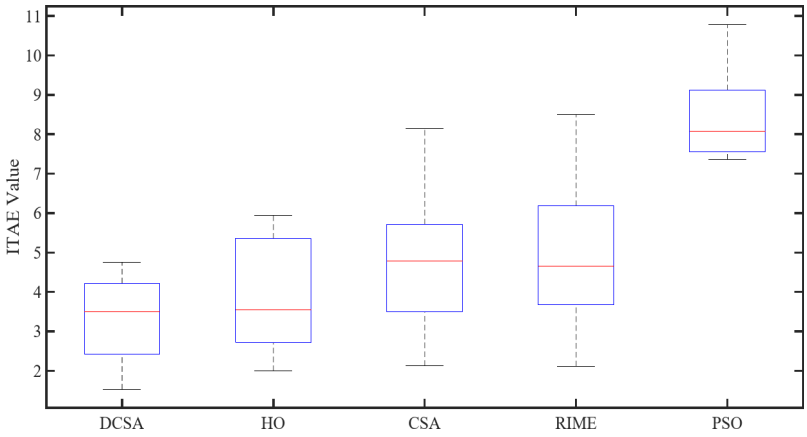


Fig. 5. Boxplots of DCSA, HO, CSA, RIME and PSO algorithms using TDn(1 + PIDn) controller.

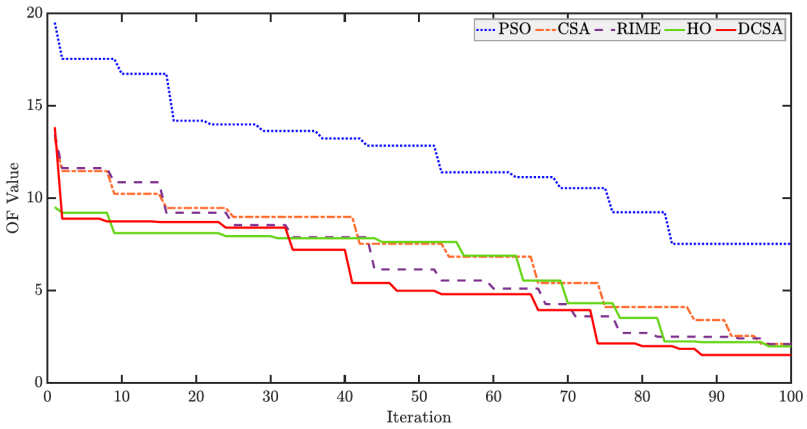


Fig. 6. Convergence profiles of DCSA, HO, CSA, RIME and PSO algorithms using TDn(1 + PIDn) controller.

Controllers – algorithms	Parameters										
	K_p	K_I	K_{PP}	K_D	N	K_{DD}	n	K_T	NN	λ	μ
TDn(1 + PIDn) – DCSA	49.9998	0.0833	0	5.8603	499.8075	5.4785	0.00035111	18.7773	653.5299	1	1
PI-PDn – EEFO[38]	15.0267	0.3086	4.8033	2.5105	198.0022	0	0	0	0	1	1
PI-PDn – QIO[12]	18.0291	0.5030	3.0402	1.5102	159.2288	0	0	0	0	1	1
PI-PDn – KMA[11]	18.3528	0.3934	4.0874	1.9076	258.4675	0	0	0	0	1	1
PI-PDn – GEO[10]	10.6192	0.5043	2.8962	1.5932	344.9394	0	0	0	0	1	1
PI-PDn – SMA[9]	16.7743	0.4045	4.0453	1.8476	209.6003	0	0	0	0	1	1
FOPID – en-CSA[8]	5.5547	0.9190	0	1.9675	0	0	0	0	0	1.0005	0.9332
FOPID – CSA[8]	5.2449	0.8503	0	1.2131	0	0	0	0	0	1.0022	0.9157
FOPID – RIME[8]	5.7250	1.1871	0	1.7104	0	0	0	0	0	0.9958	0.8054
PI – GWO[17]	4.47	0.89	0	0	0	0	0	0	0	1	0
PI – GA[17]	8.53	0.91	0	0	0	0	0	0	0	1	0
PI – PSO[17]	7.07	1.04	0	0	0	0	0	0	0	1	0

Table 4. Optimal gains of the proposed controller compared to other controllers.

in turn has an effect on the condensation process and the thermal efficiency of the system. In a similar vein, the temperature of the water that is being cooled is an important aspect that has an effect on the condenser's capacity to keep the pressure and temperature at the appropriate level for efficient functioning.

In addition, in order to develop and validate effective control strategies, it is vital to have a full understanding of how these parameters interact with one another. For the purpose of ensuring correct control of the condenser pressure, the multistage TDn(1 + PIDn) controller, which was improved by DCSA, is dependent on performing

Parameters	Value	Explanation
R	0.461526 kJ/(kgK)	Specific gas constant
V	3 m^3	Volume of the system
λ	2265.65 kJ/kg	Latent heat of vaporization
UA	356.972 kW/K	Overall heat transfer coefficient multiplied by surface area
M_{cw}	6500 kg	Mass of cooling water
C_p	4.2 kJ/(kgK)	Specific heat capacity of water
α	0.3162 K/kPa	Temperature coefficient per pressure unit
β	68.0958 °C	Temperature constant
α_1	0.087292	Coefficient for first variable term
α_2	0.00073787	Coefficient for second variable term
F_s	4 kg/s	Steam flow rate
F_c	4 kg/s	Condensate flow rate
F_{cw}	107.8881 kg/s	Cooling water flow rate
P	90 kPa	Pressure inside the system
T	80 °C	System temperature
T_{cw}	60 °C	Cooling water temperature
T_c	96.5538 °C	Condensate temperature
Q	9062.6 kW	Heat transfer rate

Table 5. Key parameters and variables of the steam condenser system.

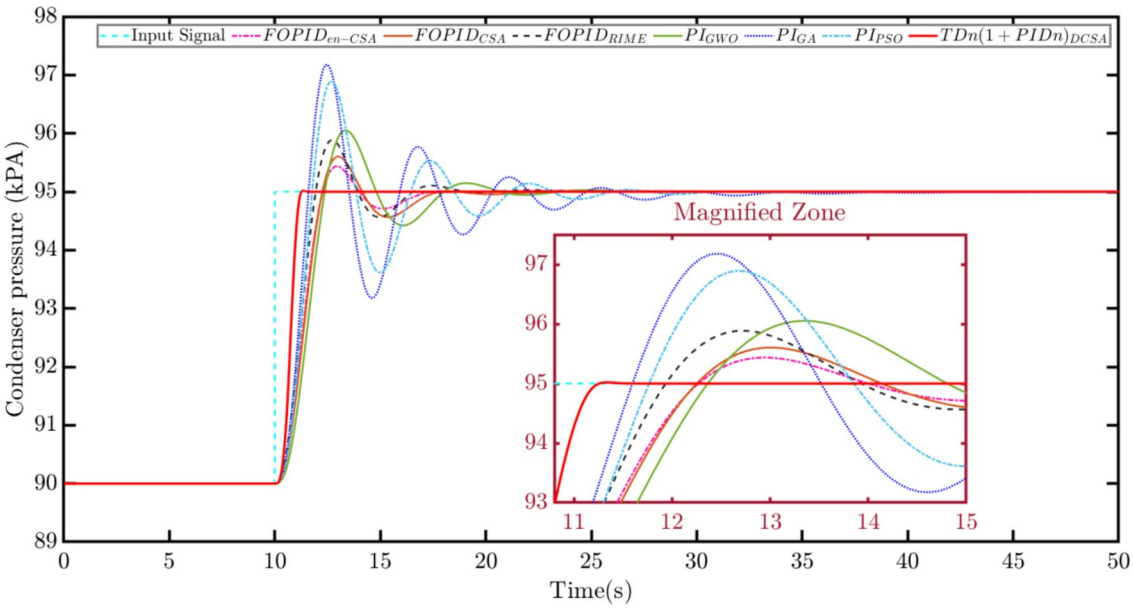


Fig. 7. Transient response for proposed DCSA-TDn(1 + PIDn) and en-CSA-FOPID, CSA-FOPID, RIME-FOPID, GWO-PI, GA-PI and PSO-PI.

precise parameter modeling. It is possible that the operation of the controller could be hindered by any deviations or errors in these parameters, which would result in pressure regulation that is less than optimal and possibly instability in the system.

As a result, the subsequent simulation analyses are based on the complete parameter listing that is presented in Table 5. It is possible for us to guarantee that the simulation results adequately reflect the behavior of the steam condenser system in the actual world if we clearly define and comprehend these factors. This, in turn, makes it possible to conduct a more trustworthy evaluation of the DCSA-optimized TDn(1 + PIDn) controller's efficiency in regulating the pressure of the condenser and enhancing the overall performance of the system.

Comparison with previous researches

The performance of the DCSA-based TDn(1 + PIDn) controller was further validated by comparing it with documented studies that employed various control strategies, including en-CSA-based FOPID, CSA-based FOPID, RIME-based FOPID, GWO-based PI, GA-based PI, and PSO-based PI. As shown in Fig. 7, the time

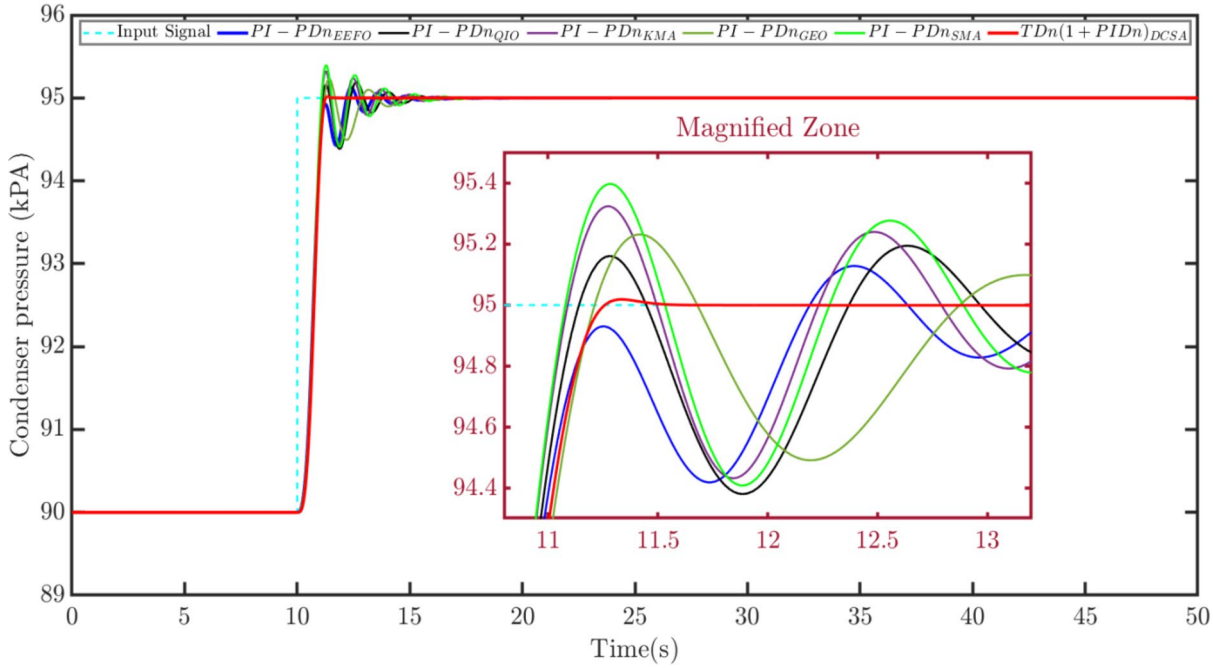


Fig. 8. Transient response for proposed DCSA-TDn(1 + PIDn) and EEFO-PI-PDn, QIO-PI-PDn, KMA-PI-PDn, GEO-PI-PDn and SMA-PI-PDn.

Controllers – algorithms	Rise time (s)	Settling time (s)	Peak time (s)	Overshoot (%)	Steady-state error (kPA)	ITAE (t_{fult}=10s and t_{sim} = 50s)
TDn(1 + PIDn) – DCSA	0.6279	11.1746	11.3349	0.3715	1.4335E – 05	1.5200
PI-PDn – EEFO[38]	0.6451	13.1799	12.3907	2.5609	5.7304E – 07	2.6957
PI-PDn – QIO[12]	0.6216	13.5744	12.6384	3.8836	4.7256E – 04	3.4737
PI-PDn – KMA[11]	0.5979	13.7774	11.2689	6.4680	2.4718E – 04	3.2355
PI-PDn – GEO[10]	0.6815	14.1196	11.4138	4.6208	1.6505E – 04	3.3463
PI-PDn – SMA[9]	0.5937	13.9776	11.2872	7.9315	5.3114E – 04	3.7972
FOPID – en-CSA[8]	1.4095	16.5104	12.9427	8.7070	4.5115E – 04	12.3398
FOPID – CSA[8]	1.4025	17.0509	13.0061	12.0526	6.5730E – 04	14.3100
FOPID – RIME[8]	1.2115	17.6610	12.7197	17.7156	0.0053	15.9775
PI – GWO[17]	1.4436	19.8228	13.3639	21.0680	1.0680E – 04	23.8138
PI – GA[17]	0.9427	28.2457	12.4960	43.5800	0.0059	64.5673
PI – PSO[17]	1.0513	24.9358	12.6667	37.8753	5.6043E – 04	43.0814

Table 6. Comparative normalized values of different time response metrics using previous researches.

response of the condenser under the DCSA-based TDn(1 + PIDn) controller is compared to those from previous studies. The results demonstrate that the DCSA-based controller provides faster and more stable responses, showcasing its superior ability to manage the nonlinear dynamics of the steam condenser effectively.

In addition, to evaluate the proposed controller and ensure proper performance, we compared this proposed controller with more powerful controller tuned by newer optimization methods. The performance of the DCSA-based TDn(1 + PIDn) controller was further validated by comparing it with documented studies that employed PI-PDn controller tuned by EEFO, QIO, KMA, GEO and SMA optimization techniques. As shown in Fig. 8, the time response of the condenser under the DCSA-based TDn(1 + PIDn) controller is compared to those from previous studies.

Transient response analysis

Table 6 provides a detailed analysis of the time response during critical periods. While the rise time is similar across all methods, the DCSA-based TDn(1 + PIDn) controller stands out by significantly reducing settling time, overshoot, rise time, and peak time. This highlights the controller's ability to deliver not only a fast response but also enhanced stability and precision. Such performance is essential for maintaining the desired pressure levels in the steam condenser without imposing excessive stress on the system. In industrial applications, this level of control is particularly critical for the precise regulation of process variables, preventing equipment damage

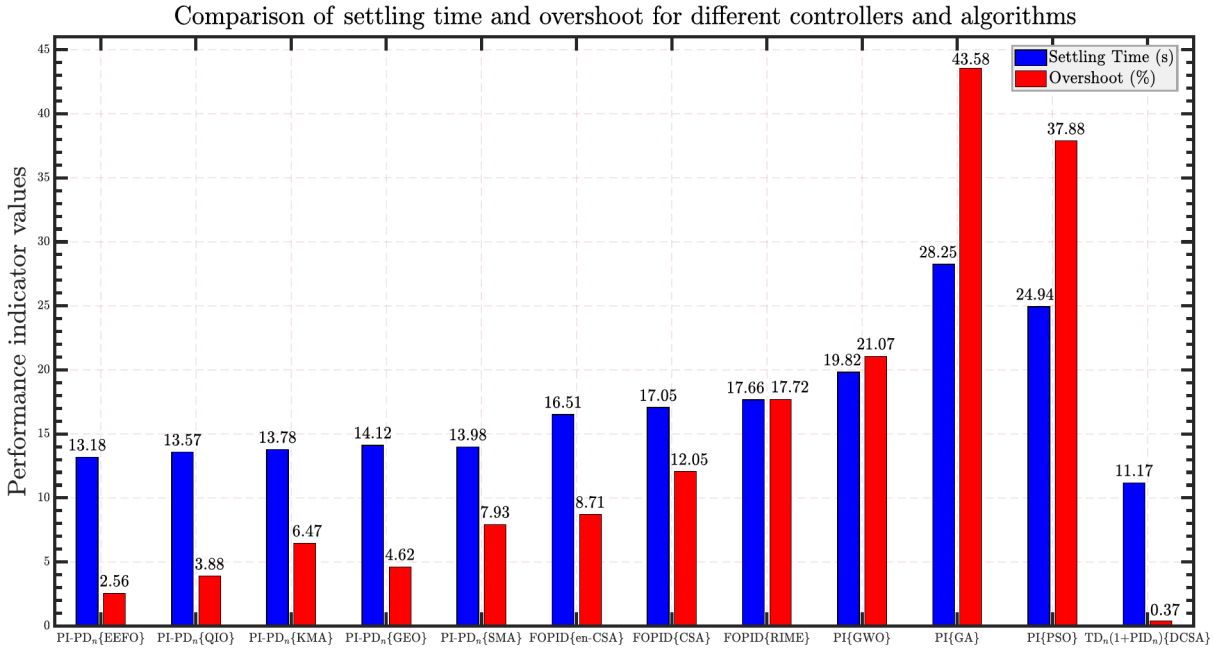


Fig. 9. Comparison of settling time and overshoot for proposed and other controllers.

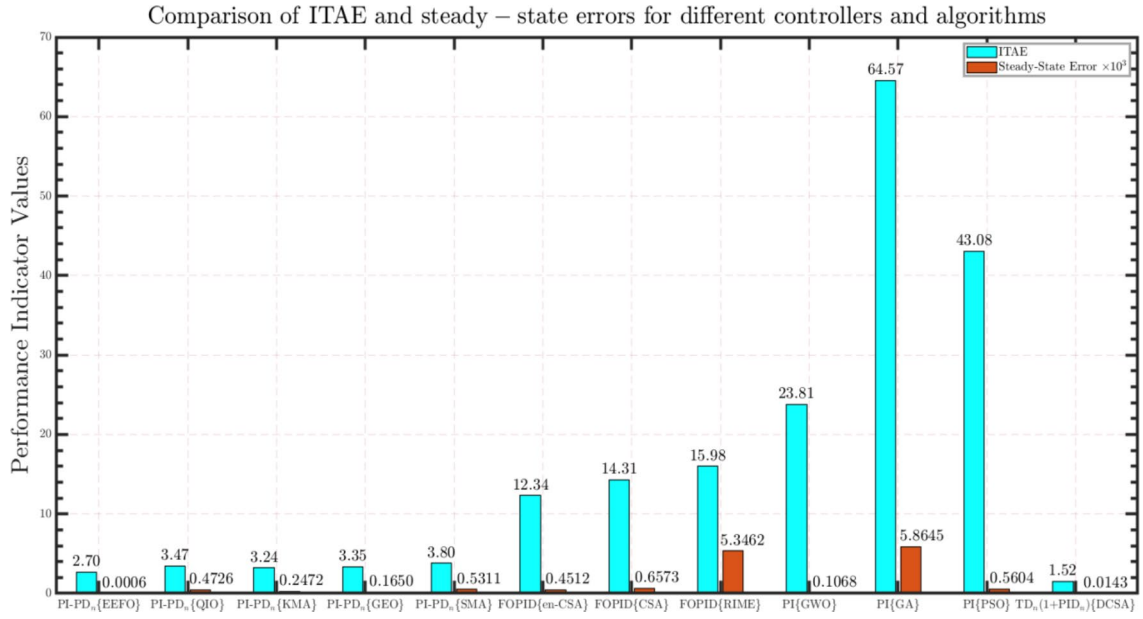


Fig. 10. Comparison of ITAE and steady-state error for proposed and other controllers.

and ensuring consistent product quality. Figures 9, 10 and 11 present a comparison of transient response values between the proposed controller and other control strategies.

Frequency response analysis

The gain, phase margins, and bandwidth are key factors in evaluating how well a controller performs, particularly in terms of stability and responsiveness. In Figs. 12 and 13, we can see the Bode plots for the shell-and-tube steam condenser system when using the proposed TDn(1 + PIDn) controller. These results are further detailed in Table 7, which compares the TDn(1 + PIDn) controller with other popular methods like FOPID, PI-PDn, and PI controllers.

The Bode diagram clearly shows that the TDn(1 + PIDn) controller excels in both robustness and speed. Its robustness is demonstrated by better gain and phase margins, meaning the system remains stable even when there are changes or disturbances. This is critical for ensuring consistent and reliable operation across

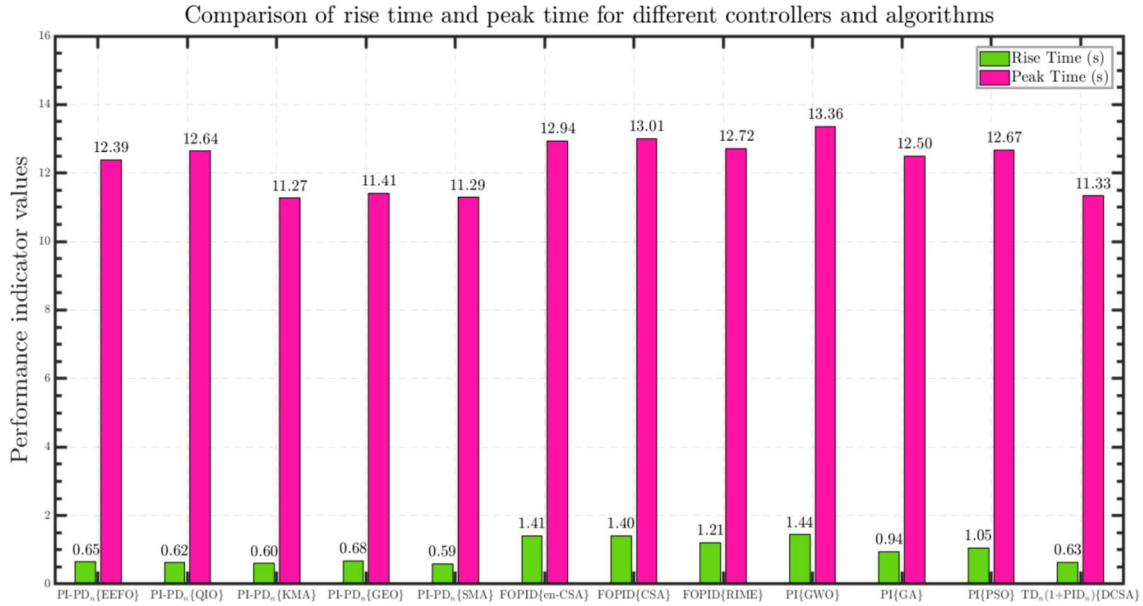


Fig. 11. Comparison of rise time and peak time for proposed and other controllers.

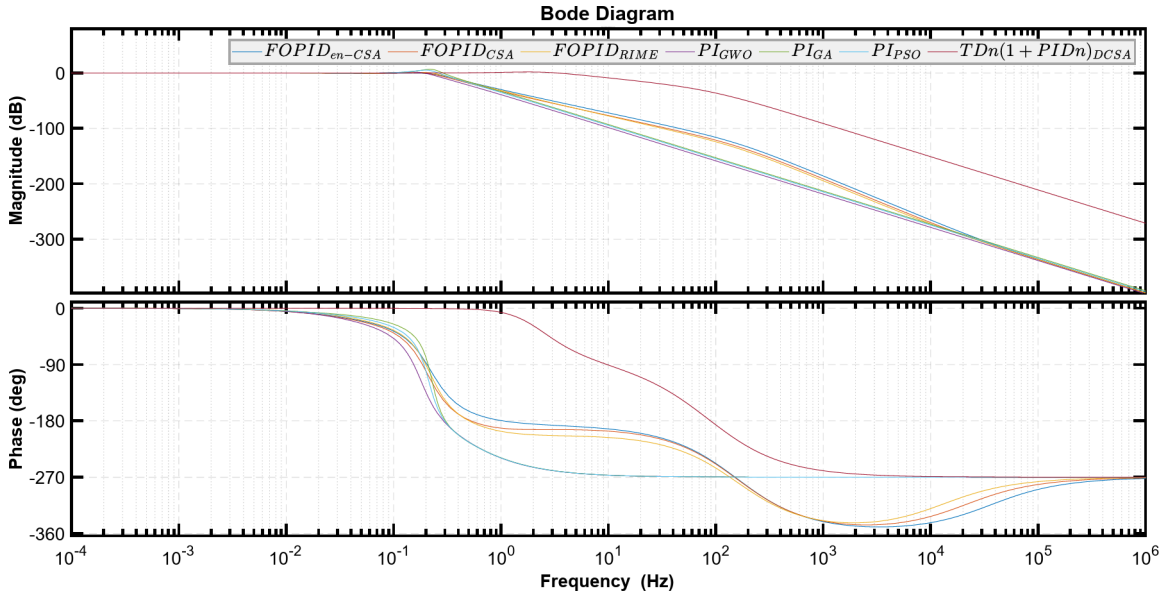


Fig. 12. Frequency response for proposed DCSA-TDn(1 + PIDn) and en-CSA-FOPID, CSA-FOPID, RIME-FOPID, GWO-PI, GA-PI and PSO-PI.

different scenarios. At the same time, the higher bandwidth of the TDn(1 + PIDn) controller translates into faster responses to system changes. Unlike the other controllers, which might lag or struggle to keep up, this approach adapts quickly and effectively. Together, these qualities make the TDn(1 + PIDn) a stronger choice overall, offering both the stability and quick reaction time needed for demanding applications.

Impact of time delay on system dynamics

This section examines how treating time delay (TD) as a nonlinear factor influences system dynamics. The system's responses to this challenging factor are analyzed, highlighting its impact on overall performance. TDs are shown to increase oscillations and complicate system stabilization. Although the system ultimately stabilizes, the nonlinear nature of time delay slows down the damping process, causing prolonged oscillations before stability is achieved. Here, it is assumed that the control system's excitation signal experiences a delay of approximately 20 *ms*. As illustrated in Figs. 14 and 15, the proposed controller demonstrates exceptional performance even in the presence of time delay. Despite the challenges posed by TD, the controller effectively

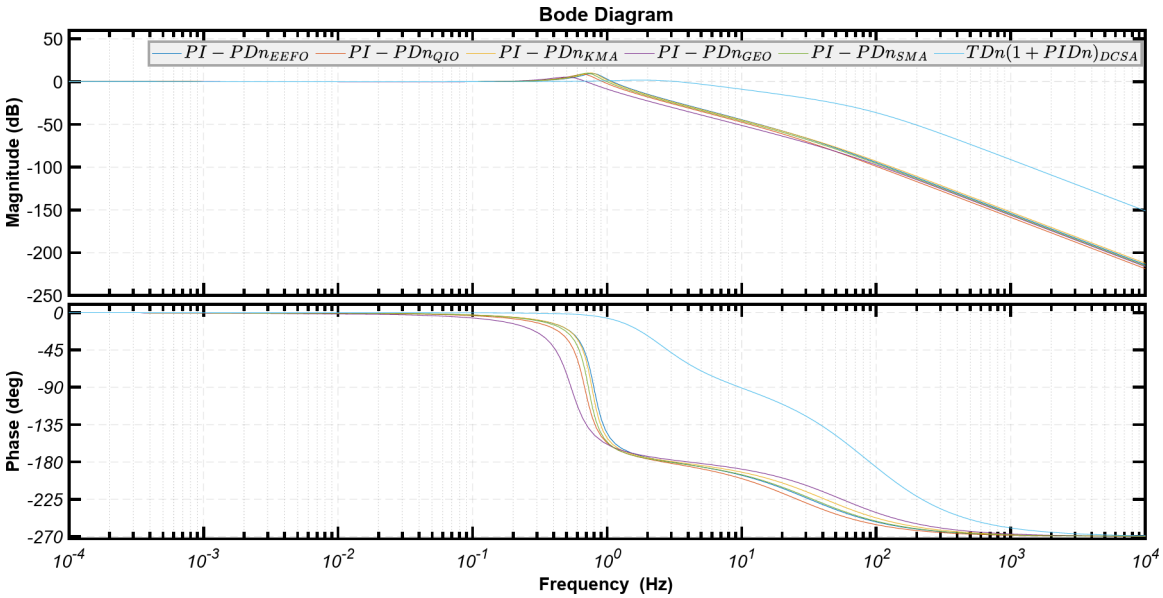


Fig. 13. Frequency response for proposed DCSA-TDn(1 + PIDn) and EEFO-PI-PDn, QIO-PI-PDn, KMA-PI-PDn, GEO-PI-PDn and SMA-PI-PDn.

Controller-Algorithm	Gain margin (dB)	Phase margin (deg.)	Bandwidth (rad/s)
TDn(1 + PIDn) – DCSA	51.55	126.88	561.92
PI-PDn – EEFO[38]	13.384	25.415	18.8
PI-PDn – QIO[12]	14.106	28.6	16.383
PI-PDn – KMA[11]	16.589	23.731	20.043
PI-PDn – GEO[10]	56.784	45.118	25.216
PI-PDn – SMA[9]	14.641	24.175	17.796
FOPID – en-CSA[8]	34.161	Infinite	6.5479
FOPID – CSA[8]	9.4315	92.454	3.2902
FOPID – RIME[8]	6.8387	72.798	3.1641
PI – GWO[17]	2.8754	54.468	1.8273
PI – GA[17]	1.2349	7.1296	1.9092
PI – PSO[17]	1.5882	17.385	1.8736

Table 7. Frequency response characteristics of proposed and different controllers.

mitigates its effects, enhancing system stability and expediting the damping of oscillations. Table 8 provides a detailed analysis of the time response during this scenario.

Input signal tracking performance

Accurate input signal tracking is crucial for maintaining optimal system performance, particularly in dynamic environments. We compared the proposed controller's tracking ability with the best controllers from recent studies. As shown in Fig. 16, the DCSA-based TDn(1 + PIDn) controller demonstrates superior accuracy in tracking input signals, significantly outperforming the EEFO-based PI-PDn controller. Figure 17 further highlights the performance of the proposed controller across different regions and conditions, with magnified sections illustrating its effectiveness. Maintaining this level of precision is critical for ensuring process stability and achieving desired outcomes in real-time applications.

Impact of non-ideal conditions on the performance of the proposed DCSA-based TDn(1 + PIDn) controller

To evaluate the robustness of the proposed control strategy, the performance of the DCSA-based TDn(1 + PIDn) controller was tested under non-ideal conditions, including external disturbances and random noise. Figure 18 demonstrates the inclusion of those conditions. An external disturbance signal (Dist(s)) and noise signal (N(s)) were introduced to the system to replicate real-world operating conditions that could impact the system's stability and control accuracy. The disturbance signal Dist(s) represents external forces or influences that might

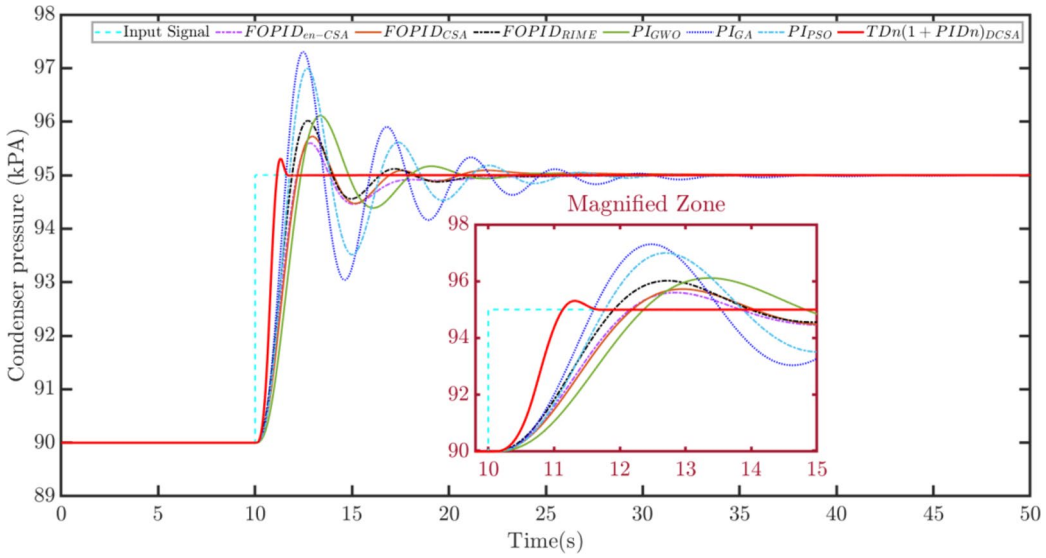


Fig. 14. Transient response for proposed DCSA-TDn(1 + PIDn) and en-CSA-FOPID, CSA-FOPID, RIME-FOPID, GWO-PI, GA-PI and PSO-PI with time delay.

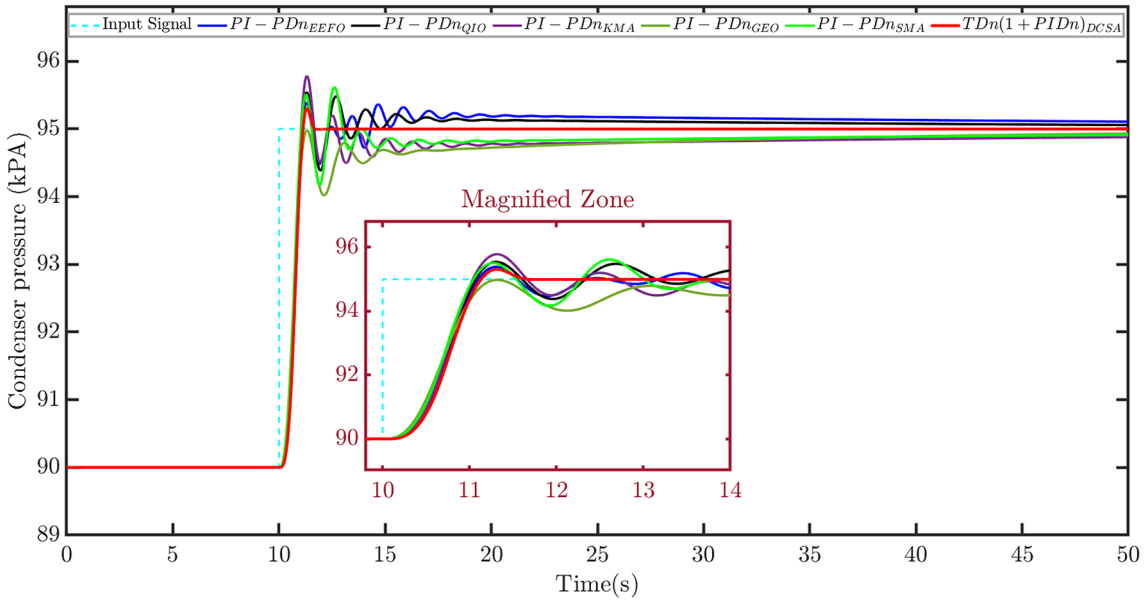


Fig. 15. Transient response for proposed DCSA-TDn(1 + PIDn) and EEFO-PI-PDn, QIO-PI-PDn, KMA-PI-PDn, GEO-PI-PDn and SMA-PI-PDn with time delay.

affect system behavior, while the noise signal N(s) was modeled as uniformly distributed random noise within the range of [− 0.01, 0.01] kPA, with a sample time of 0.1 s.

These perturbations were applied to assess the controller's capability to maintain stability and precise pressure control despite such disruptions. Additionally, saturation limits of [− 50, 50] were imposed to reflect the physical constraints of the actuator, ensuring that control actions remained within practical operational limits. The design of the control system, illustrating how the external disturbance Dist(s) and noise signal N(s) were incorporated into the simulation environment, is shown in Fig. 19. The integration of these factors ensures a more realistic evaluation of the controller's performance under challenging conditions, providing a thorough assessment of its robustness and stability in the face of real-world operational disruptions.

Closed-loop behavior of the proposed DCSA-based TDn(1 + PIDn) controller

The closed-loop response of the proposed control strategy was evaluated to verify the controller's effectiveness under varying operational conditions, such as fluctuations in circulating water outlet temperature, cooling water flow, and steam heat. As shown in Fig. 20, the DCSA-based TDn(1 + PIDn) controller successfully maintains

Controllers – algorithms	Rise time (s)	Settling time (s)	Peak time (s)	Overshoot (%)	Steady-state error (kPA)	ITAE (t_{fult}=10s and t_{sim} = 50s)
TDn(1 + PIDn) – DCSA	0.5944	11.5334	11.3105	6.1763	0.0013	2.6319
PI-PDn – EEFO[38]	0.5926	28.5145	11.2998	7.7778	0.1065	114.2665
PI-PDn – QIO[12]	0.5861	29.9615	11.3085	10.8742	0.0577	70.5483
PI-PDn – KMA[11]	0.5659	30.5412	11.3218	15.6711	0.1207	132.2868
PI-PDn – GEO[10]	0.6970	41.8277	11.3192	0	0.0685	114.5886
PI-PDn – SMA[9]	0.5819	44.6325	12.6112	12.3485	0.0880	101.0055
FOPID – en-CSA[8]	1.3327	19.5477	12.8435	11.9885	0.0232	20.1607
FOPID – CSA[8]	1.3535	19.7273	12.9528	14.4682	0.0012	23.6769
FOPID – RIME[8]	1.1811	20.1017	12.7233	20.3463	0.0058	19.7495
PI – GWO[17]	1.4292	19.9418	13.3620	22.2707	1.0520E – 04	25.3553
PI – GA[17]	0.9326	28.4316	12.5014	46.1104	0.0063	73.1582
PI – PSO[17]	1.0419	25.1380	12.6710	39.9199	4.7752E – 04	48.4817

Table 8. Comparative normalized values of different time response metrics using previous researches with time delay.

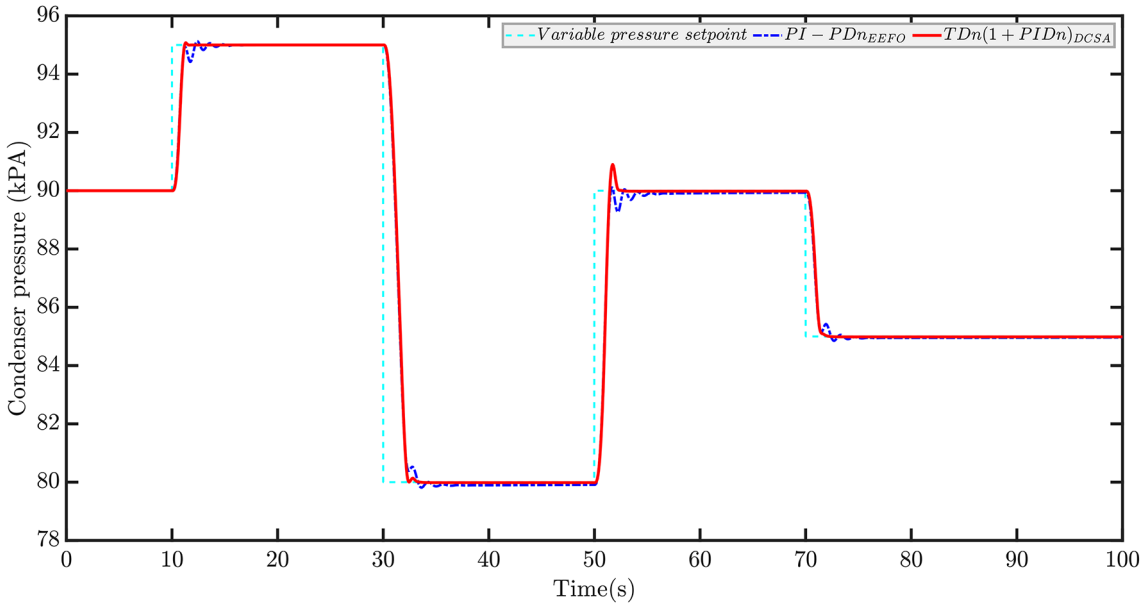


Fig. 16. Performance of the proposed controller and en-CSA-FOPID in terms of input signal tracking.

system stability while achieving the desired control objectives, even in dynamic scenarios. Its ability to adapt to changes in key process variables without compromising control performance is essential for ensuring the long-term reliability and efficiency of the steam condenser system.

Conclusions and future works

This study introduces a novel multistage controller, TDn(1 + PIDn), optimized through the DCSA, to address the challenges of controlling nonlinear shell-and-tube steam condensers. The TDn(1 + PIDn) controller is specifically designed to manage system nonlinearities, mitigate external disturbances, and fine-tune multiple control parameters typical in thermal power plant operations. By leveraging the capabilities of DCSA, the proposed controller achieves significant improvements in system performance, including enhanced stability, faster settling and rise times, reduced peak times and overshoot, and minimized steady-state errors. These attributes make it a robust and reliable solution for controlling complex nonlinear industrial systems. The effectiveness of the TDn(1 + PIDn) controller was validated through extensive simulations, demonstrating its superiority over several advanced metaheuristic algorithms, such as GA, PSO, GWO, RIME, CSA, en-CSA, EEFO, SMA, GEO, KMA, and QIO. Performance comparisons showed that the DCSA-based controller consistently outperformed other strategies in optimizing the ITAE objective function, achieving better transient and steady-state responses under a wide range of operating conditions. Further evaluation of the controller under challenging scenarios, including external disturbances and system noise, confirmed its robustness and resilience. Unlike conventional methods, the DCSA-based controller maintained superior performance, reinforcing its adaptability and reliability in dynamic and uncertain environments. The comparative analysis

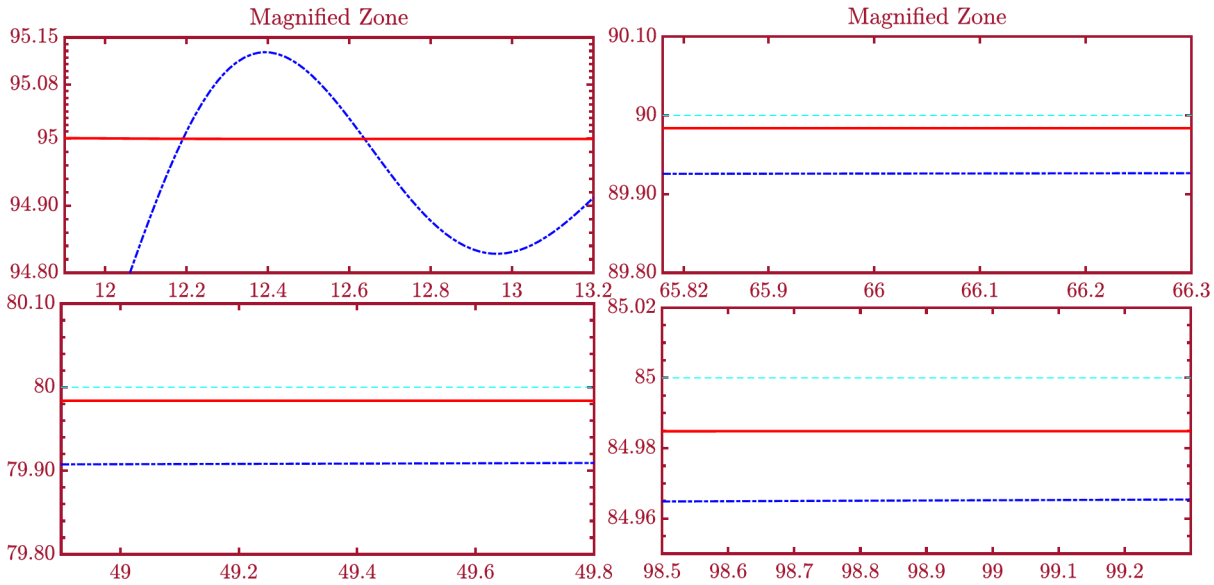


Fig. 17. Magnified zone performance of the proposed controller and en-CSA-FOPID in terms of input signal tracking.

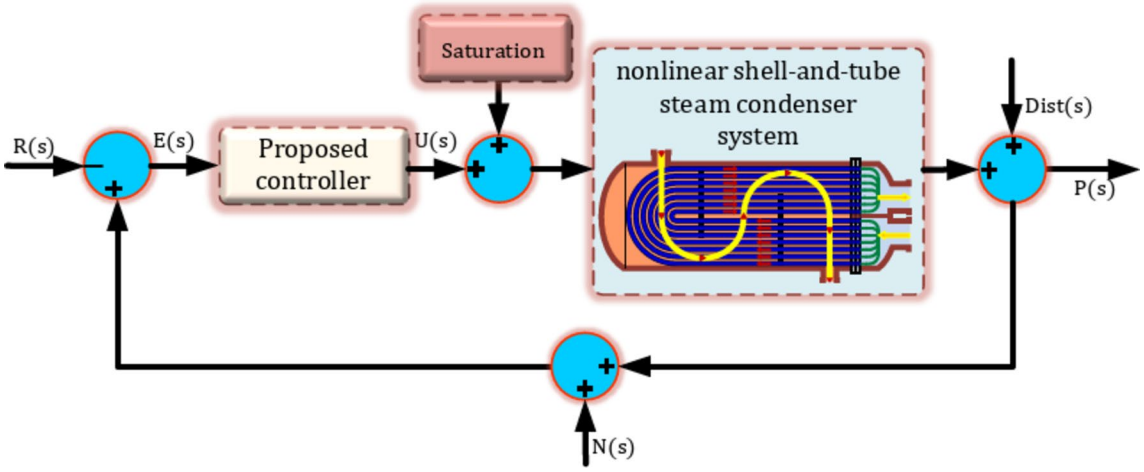


Fig. 18. Schematic of the proposed control system for saturation and disturbances.

with existing studies underscored the effectiveness of the DCSA algorithm as a powerful optimization tool, enhancing the performance and reliability of control systems. This research makes a significant contribution to the field of industrial control systems, particularly in thermal power plant applications. It not only validates the applicability of the DCSA algorithm for optimizing control in nonlinear systems but also highlights its potential for broader applications. By addressing the critical challenges of pressure regulation in steam condensers, this study paves the way for future exploration of bio-inspired optimization techniques and advanced multistage control strategies for other complex, nonlinear systems.

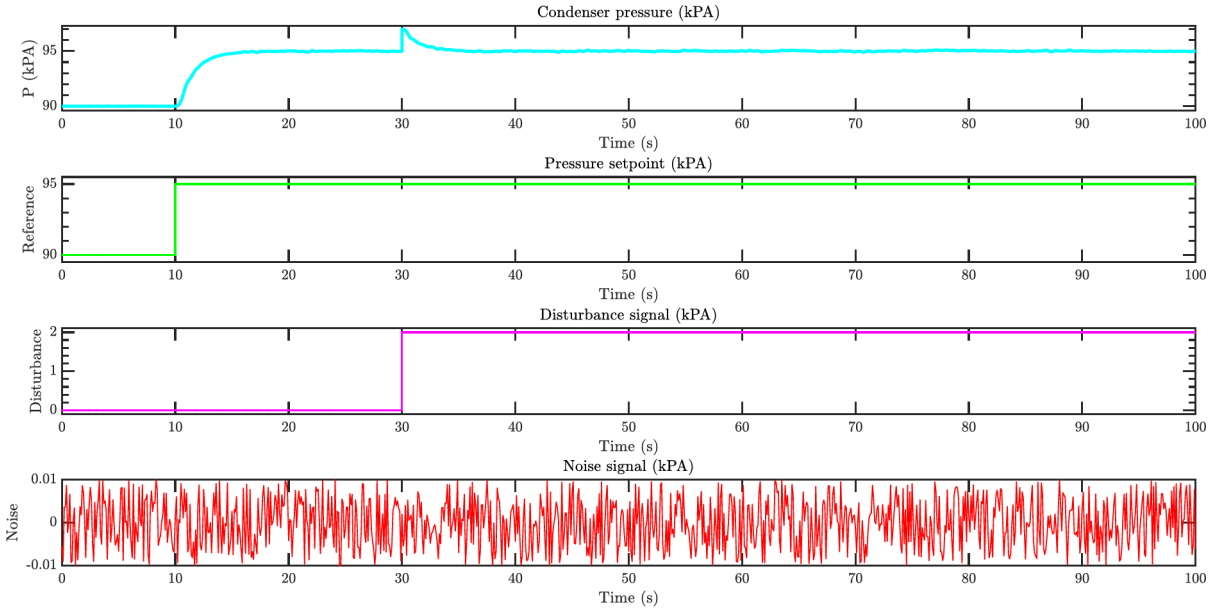


Fig. 19. Performance of the proposed approach with respect to noise and disturbance effects.

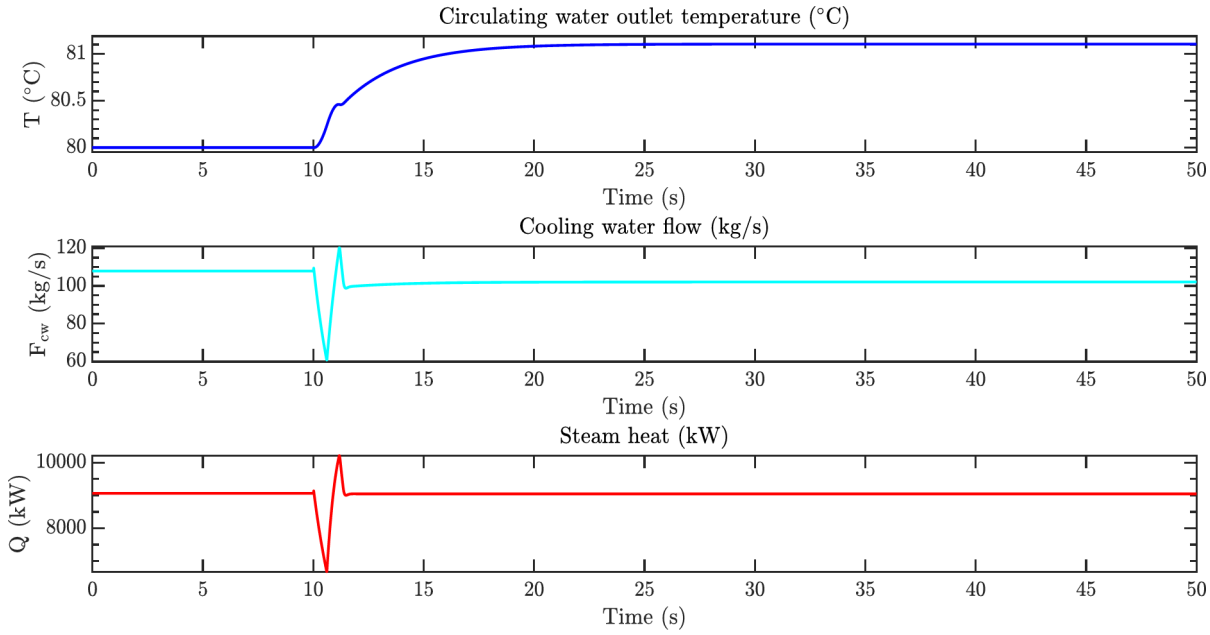


Fig. 20. Closed-loop response of the proposed control strategy with respect to circulating water outlet temperature, cooling water flow and steam heat.

Data availability

The datasets used and/or analysed during the current study available from the corresponding author on reasonable request.

Received: 20 October 2024; Accepted: 8 January 2025
Published online: 15 January 2025

References

1. Wang, Z., Liu, M., Yan, H. & Yan, J. Optimization on coordinate control strategy assisted by high-pressure extraction steam throttling to achieve flexible and efficient operation of thermal power plants. *Energy* **244**, 122676 (2022).
2. Khaleel, O. J., Basim Ismail, F., Khalil Ibrahim, T. & bin Abu Hassan, S. H. Energy and exergy analysis of the steam power plants: a comprehensive review on the classification, Development, improvements, and configurations. *Ain Shams Eng. J.* **13**, 101640 (2022).

3. Madejski, P., Kuś, T., Michalak, P., Karch, M. & Subramanian, N. Direct contact condensers: a Comprehensive Review of Experimental and Numerical investigations on Direct-Contact Condensation. *Energies (Basel)* **15**, 9312 (2022).
4. Ni, L., Li, Y., Zhang, L. & Wang, G. A modified aquila optimizer with wide plant adaptability for the tuning of optimal fractional proportional–integral–derivative controller. *Soft Comput.* **28**, 6269–6305 (2024).
5. Sagor, A. R. et al. Pelican optimization algorithm-based proportional–integral–derivative Controller for Superior frequency regulation in interconnected Multi-area Power Generating System. *Energies (Basel)* **17**, 3308 (2024).
6. Gulzar, M. M., Sibtain, D. & Khalid, M. Innovative design for enhancing transient stability with an ATFOPID controller in hybrid power systems. *J. Energy Storage* **99**, 113364 (2024).
7. Qu, Z. et al. Optimized PID Controller for load frequency control in multi-source and Dual-Area Power Systems Using PSO and GA algorithms. *IEEE Access.* 1–1. https://doi.org/10.1109/ACCESS.2024.3445165 (2024).
8. Alzakari, S. A., Izci, D., Ekinci, S., Alhussan, A. A. & Hashim, F. A. Nonlinear FOPID controller design for pressure regulation of steam condenser via improved metaheuristic algorithm. *PLoS One* **19**, e0309211 (2024).
9. Li, S., Chen, H., Wang, M., Heidari, A. A. & Mirjalili, S. Slime mould algorithm: a new method for stochastic optimization. *Future Generation Comput. Syst.* **111**, 300–323 (2020).
10. Mohammadi-Balani, A., Dehghan Nayeri, M., Azar, A. & Taghizadeh-Yazdi, M. Golden eagle optimizer: a nature-inspired metaheuristic algorithm. *Comput. Ind. Eng.* **152**, 107050 (2021).
11. Suyanto, S., Ariyanto, A. A. & Ariyanto, A. F. Komodo Mlipir Algorithm. *Appl. Soft Comput.* **114**, 108043 (2022).
12. Zhao, W. et al. Quadratic interpolation optimization (QIO): a new optimization algorithm based on generalized quadratic interpolation and its applications to real-world engineering problems. *Comput. Methods Appl. Mech. Eng.* **417**, 116446 (2023).
13. Muni, M. K., Parhi, D. R. & Kumar, P. B. Implementation of grey wolf optimization controller for multiple humanoid navigation. *Comput. Animat Virtual Worlds* **31**, (2020).
14. Shami, T. M. et al. Particle swarm optimization: a Comprehensive Survey. *IEEE Access.* **10**, 10031–10061 (2022).
15. Parvin, K. et al. Intelligent Controllers and Optimization Algorithms for Building Energy Management towards Achieving Sustainable Development: challenges and prospects. *IEEE Access.* **9**, 41577–41602 (2021).
16. Deng, W., Xu, J. & Zhao, H. An Improved ant colony optimization Algorithm based on hybrid strategies for Scheduling Problem. *IEEE Access.* **7**, 20281–20292 (2019).
17. Li, S. X. & Wang, J. S. Dynamic modeling of Steam Condenser and Design of PI Controller based on Grey Wolf Optimizer. *Math. Probl. Eng.* **2015**, 1–9 (2015).
18. Mishra, D., Nayak, P. C., Bhoi, S. K. & Prusty, R. C. Design and analysis of Multi-stage TDF/(1 + TI) controller for Load-frequency control of A.C Multi-Islanded Microgrid system using Modified Sine cosine algorithm. in *1st Odisha International Conference on Electrical Power Engineering, Communication and Computing Technology(ODICON)* 1–6 (IEEE, 2021). https://doi.org/10.1109/ODICON50556.2021.9428969 (2021).
19. Wang, J. S. & Li, S. X. PID Controller of Steam Condenser based on particle swarm optimization algorithm. *J. Comput. Theor. Nanosci.* **14**, 3698–3701 (2017).
20. Idir, A. et al. PID Controller Design with a New Method Based on Fractionalized Integral Gain for Cruise Control System. in. *IEEE International Conference on Environment and Electrical Engineering and 2024 IEEE Industrial and Commercial Power Systems Europe (EEEIC / I&CPS Europe)* 1–6 (IEEE, 2024). https://doi.org/10.1109/EEEIC/ICPSEurope61470.2024.10751521 (2024).
21. Jabari, M., Izci, D., Ekinci, S., Bajaj, M. & Zaitsev, I. Performance analysis of DC-DC Buck converter with innovative multi-stage PIDn(1 + PD) controller using GEO algorithm. *Sci. Rep.* **14**, 25612 (2024).
22. Bin Roslan, M. N., Bingi, K., Devan, P. A. M. & Ibrahim, R. Design and development of Complex-Order PI-PD controllers: Case studies on pressure and Flow process control. *Appl. Syst. Innov.* **7**, 33 (2024).
23. Jabari, M., Ekinci, S., Izci, D., Bajaj, M. & Zaitsev, I. Efficient DC motor speed control using a novel multi-stage FOPD(1 + PI) controller optimized by the Pelican optimization algorithm. *Sci. Rep.* **14**, 22442 (2024).
24. Jabari, M. & Rad, A. Optimization of Speed Control and Reduction of Torque Ripple in switched Reluctance motors using Metaheuristic algorithms based PID and FOPID controllers at the Edge. *Tsinghua Sci. Technol.* https://doi.org/10.26599/TST.2024.9010021 (2024).
25. Idir, A., Bensafia, Y. & Canale, L. Influence of approximation methods on the design of the novel low-order fractionalized PID controller for aircraft system. *J. Brazilian Soc. Mech. Sci. Eng.* **46**, 98 (2024).
26. Elkasem, A. H. A., Kamel, S., Khamies, M. & Nasrat, L. Frequency regulation in a hybrid renewable power grid: an effective strategy utilizing load frequency control and redox flow batteries. *Sci. Rep.* **14**, 9576 (2024).
27. Hassan, A. et al. Optimized Multiloop Fractional-Order Controller for regulating frequency in diverse-sourced vehicle-to-Grid Power systems. *Fractal Fract.* **7**, 864 (2023).
28. Nayak, P. C., Mishra, S., Prusty, R. C. & Panda, S. Hybrid whale optimization algorithm with simulated annealing for load frequency controller design of hybrid power system. *Soft Comput.* https://doi.org/10.1007/s00500-023-09072-1 (2023).
29. Mishra, D., Nayak, P. C., Prusty, R. C. & Panda, S. An improved equilibrium optimization-based fuzzy tilted double integral derivative with filter (F-TIDF-2) controller for frequency regulation of an off-grid microgrid. *Electr. Eng.* **106**, 2033–2055 (2024).
30. Baral, K. K., Nayak, P. C., Mohanty, B. & Barisal, A. K. Improved frequency regulation of dual-area hybrid power system with the influence of energy storage devices. *Electr. Eng.* https://doi.org/10.1007/s00202-024-02670-8 (2024).
31. Jibril, M., Tadesse, M., Hassen, N. & Abebe, Y. Modeling and Performance Analysis of Shell Tube Surface Condenser under Lumped parameters using fuzzy self-tuning PI Controller. *Int. J. Electron. Electr. Eng. Syst.* **3**, (2020).
32. Ekinci, S. et al. Optimizing steam condenser efficiency: integrating logarithmic spiral search and greedy selection mechanisms in gazelle optimizer for PI controller tuning. *Results Eng.* **24**, 103501 (2024).
33. Askarzadeh, A. A novel metaheuristic method for solving constrained engineering optimization problems: crow search algorithm. *Comput. Struct.* **169**, 1–12 (2016).
34. Amiri, M. H., Hashjin, M., Montazeri, N., Mirjalili, M., Khodadadi, N. & S. & Hippopotamus optimization algorithm: a novel nature-inspired optimization algorithm. *Sci. Rep.* **14**, 5032 (2024).
35. Su, H. et al. A physics-based optimization. *Neurocomputing* **532**, 183–214 (2023).
36. Ekinci, S. et al. Automatic Generation Control of a hybrid PV-Reheat Thermal Power System using RIME algorithm. *IEEE Access.* **12**, 26919–26930 (2024).
37. Izci, D., Ekinci, S. & Ma'arif, A. Parameter extraction of triple-diode Photovoltaic Model via RIME Optimizer with Neighborhood Centroid Opposite Solution. *J. Rob. Control (JRC)* **5**, 1098–1103 (2024).
38. Zhao, W. et al. Electric eel foraging optimization: a new bio-inspired optimizer for engineering applications. *Expert Syst. Appl.* **238**, 122200 (2024).

Acknowledgements

This article has been produced with the financial support of the European Union under the REFRESH – Research Excellence For Region Sustainability and High-tech Industries project number CZ.10.03.01/00/22_003/0000048 via the Operational Programme Just Transition and paper was supported by the following project TN02000025 National Centre for Energy II. The authors would like to express their sincere gratitude to Stanislav Misak for his exceptional supervision, project administration, and overall guidance throughout the course of this project. His

expertise and support were instrumental to its success.

Author contributions

Mostafa Jabari, Serdar Ekinci: Conceptualization, Methodology, Software, Visualization, Investigation, Writing-Original draft preparation. Davut Izci: Data curation, Validation, Supervision, Resources, Writing - Review & Editing. Mohit Bajaj, Lukas Prokop, Vojtech Blazek: Project administration, Supervision, Resources, Writing - Review & Editing.

Declarations

Competing interests

The authors declare no competing interests.

Additional information

Correspondence and requests for materials should be addressed to M.B.

Reprints and permissions information is available at www.nature.com/reprints.

Publisher's note Springer Nature remains neutral with regard to jurisdictional claims in published maps and institutional affiliations.

Open Access This article is licensed under a Creative Commons Attribution-NonCommercial-NoDerivatives 4.0 International License, which permits any non-commercial use, sharing, distribution and reproduction in any medium or format, as long as you give appropriate credit to the original author(s) and the source, provide a link to the Creative Commons licence, and indicate if you modified the licensed material. You do not have permission under this licence to share adapted material derived from this article or parts of it. The images or other third party material in this article are included in the article's Creative Commons licence, unless indicated otherwise in a credit line to the material. If material is not included in the article's Creative Commons licence and your intended use is not permitted by statutory regulation or exceeds the permitted use, you will need to obtain permission directly from the copyright holder. To view a copy of this licence, visit http://creativecommons.org/licenses/by-nc-nd/4.0/.

© The Author(s) 2025